Free-Space Communication With Directly Modulated Mid-Infrared Quantum Cascade Devices

Olivier Spitz, Pierre Didier, Lauréline Durupt, Daniel Andrés Díaz-Thomas, Alexei N. Baranov, Laurent Cerutti, and Frédéric Grillot, *Senior Member, IEEE*

***Abstract*—This study deals with the communication capabilities of two kinds of semiconductor lasers emitting in one of the atmosphere transparency windows, around 4 μm. One of these two lasers is a quantum cascade laser and the other one is an interband cascade laser. With the quantum cascade laser, a subsequent attenuation is added to the optical path in order to mimic the attenuation of free-space transmission of several kilometers. Direct electrical modulation is used to transmit the message and two-level formats, non-return-to-zero and return-to-zero, are used and compared in terms of maximum transmission data rate. The sensitivity to optical feedback is also analyzed, as well as the evolution of the error rate when reducing the optical power at the level of the detector. This work provides a novel insight into the development of future secure free-space optical communication links based on mid-infrared semiconductor lasers and sheds the light on improvements required to achieve multi-Gbits/s communication with off-the-shelf components.**

***Index Terms*—Quantum cascade laser, interband cascade laser, mid-infrared photonics, free-space communication.**

I. Introduction

THE development of semiconductor laser technology was considerably boosted with inventing quantum cascade lasers (QCLs) in early 90s [1] and interband cascade lasers (ICLs) shortly afterwards [2]. At the early stages of QCLs, free-space optical transmissions were envisioned [3] alongside other applications such as spectroscopy [4] and high-speed detection [5]. However, the requirement for cryogenic temperatures at that time [6] hindered the development of versatile transmission systems, despite data rates already in the range of Gbits/s. A few years later, ICLs drew attention with electrical bandwidth of several GHz [7], but the communication rate was limited to 70 Mbits/s [8] and, to the best of our knowledge, no further attempt was performed since then. With the advent of new telecommunication standards and the ever increasing need for transfer speed, there has been a renewed interest in the QCL community for powerful room-temperature sources [9], high-speed modulators [10], sensitive detectors [11], structures optimized for RF-injection [12], extension to fiber networks [13] and methods to improve privacy [14], not only in the mid-infrared domain but also in the terahertz domain [15], where recent findings pave the way towards terahertz QCLs at room temperature [16], [17]. This was motivated by the limitations induced by direct electrical modulation of QCLs and ICLs at room temperature, with data rates often below 100 Mbits/s [8], [18], [19], except for one configuration with digital signal processing techniques [20]. Direct electrical modulation remains however the most versatile method to transmit a signal with a cascade laser. Besides, the numerous electrical rectification results obtained at room temperature with these semiconductor lasers [21]–[23] are in favor of higher transmission rates than those previously described. In free-space optical communication (FSO), the operating wavelength is a key parameter, and it is highly desirable to work in a configuration that is immune to the environmental parameters, such as turbulence, fog or scattering. In order to improve the FSO availability, performance and range, the investigation of the cross-relation between the climatic conditions and the wavelength is highly required [24]. QCLs and ICLs providing high performance in the mid-infrared raised attention because the atmosphere is highly transparent in two domains called mid-infrared (MIR) window between 3-5 μm and long-wave infrared (LWIR) window between 8.5-11 μm [25]. Moreover, not only the absorption but also the signal distortion is lower at higher wavelength, so the MIR and LWIR windows have a further advantage with regard to the near-infrared domain that is currently used for free-space links [26]. Indeed, it is known that turbulence on the propagation path significantly deteriorates the optical signal causing for instance beam spreading, beam wandering, scintillation or loss of spatial coherence. In this case, the scintillation will be the predominant phenomenon, corresponding to intensity fluctuations of the propagating beam.

Manuscript received April 14, 2021; revised June 7, 2021; accepted July 5, 2021. Date of publication July 13, 2021; date of current version August 16, 2021. This work was supported in part by French Defense Agency (DGA), in part by French ANR program under Grants ANR-17-ASMA-0006 and ANR-11-EQPX-0016, and in part by the European Office of Aerospace Research and Development under Grant FA9550-18-1-7001. *(Corresponding author: Olivier Spitz.)*

Olivier Spitz is with the LTCI Télécom Paris, Institut Polytechnique de Paris, 91120 Palaiseau, France (e-mail: olivier.spitz@telecom-paristech.fr).

Daniel Andrés Díaz-Thomas, Alexei N. Baranov, and Laurent Cerutti are with the Institut d'Electronique et des Systèmes, Université de Montpellier, CNRS UMR 5214, 34000 Montpellier, France (e-mail: daniel.diaz-thomas@umontpellier.fr; baranov@univ-montp2.fr; laurent.cerutti@umontpellier.fr).

Pierre Didier and Lauréline Durupt are with the LTCI Télécom Paris, Institut Polytechnique de Paris, 91120 Palaiseau, France, with the mirSense, Centre d'intégration NanoInnov, 91120 Palaiseau, France (e-mail: pierre.didier@telecom-paris.fr; laureline.durupt@mirsense.com).

Frédéric Grillot is with the LTCI Télécom Paris, Institut Polytechnique de Paris, 91120 Palaiseau, France, and also with the Center for High Technology Materials, University of New-Mexico, Albuquerque, NM 87106 USA (e-mail: frederic.grillot@telecom-paristech.fr).

Color versions of one or more figures in this article are available at https://doi.org/10.1109/JSTQE.2021.3096316.

Digital Object Identifier 10.1109/JSTQE.2021.3096316

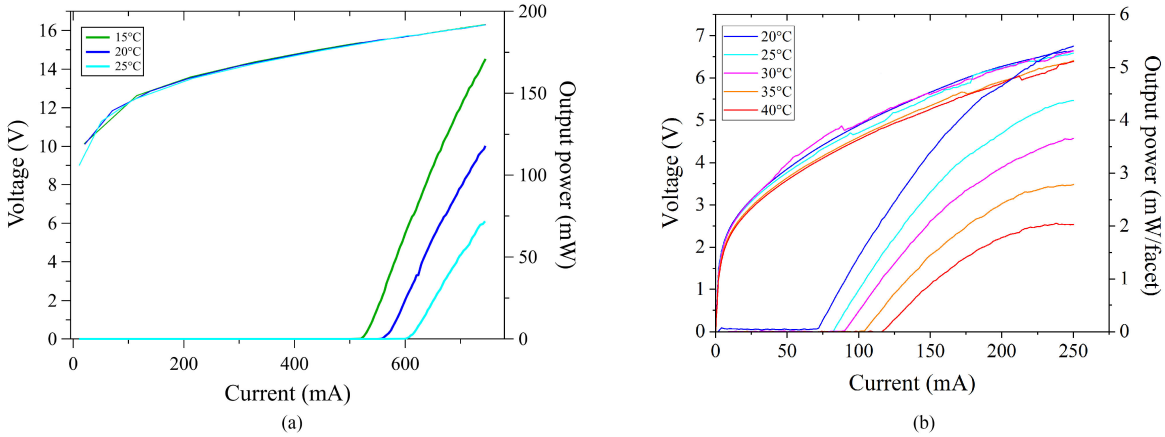

Fig. 1. Experimental Ligh-Intensity-Voltage (LIV) curves for the two lasers under continuous wave pumping and for various temperatures of operation. (a) For the packaged QCL and (b) for the ICL.

This effect evolves as a function of $\lambda^{-7/6}$ [27] and will therefore be less significant at higher wavelength, hence the advantage of the cascade lasers under study for FSO.

This paper further investigates direct electrical modulation of a QCL and an ICL for high-speed transmission, both lasers emitting in one of the transparency windows of the atmosphere, near 4 μm. Section II introduces the features of the ICL and the packaged QCL, as well as the experimental setup giving access to the bandwidth analysis and the experimental setup for the transmission with on-off-keying signals. The electrical bandwidth and the optical bandwidth of the lasers are compared and give indications about the maximum transmission rate one can expect. Section III assesses the quality of the transmission for the two lasers, by introducing eye diagrams and bit-error-rates (BER). Two different formats of modulation are tested and the one with a return-to-zero scheme gives higher rates. This section also investigates the resistance to external perturbations in the case of the packaged QCL and shows that this configuration is relevant for long-haul transmissions, even in degraded conditions. Eventually, Section IV summarizes the results and provides guidelines for future work about the implementation of a real-field experiment with mid-infrared cascade lasers.

II. Methods

A. Photonic Devices

The two devices under investigation are Fabry-Perot mid-infrared cascade semiconductor lasers emitting around the same wavelength (4 μm) but they rely on two different technologies. The first device from Alpes Lasers is a QCL, which means that lasing is achieved through intersubband transitions. This method is designed for wavelength operation up to the terahertz domain, but it is also a candidate of choice for targeting the two transparency windows of the atmosphere [28]. One of the peculiarities of QCLs is that they do not exhibit relaxation oscillations and they are thus considered very promising for very high-speed modulation [29] because usually, the relaxation frequency sets the limit for maximum direct modulation in a semiconductor laser [30]. As already described in the literature [20], we will see that other phenomena actually limit the bandwidth of our QCL and do not allow for very high-speed direct modulation, unless the laser is mounted on a dedicated RF launcher. Our QCL is inserted inside a high-heat-load (HHL) package with embedded focusing lens and Peltier-cooled system. The threshold current is 515 mA and the maximum output power is 170 mW at 288 K, as seen in Fig. 1(a). This QCL is a high-power optical source but it consumes a lot of electrical power (16.5 V and 750 mA at maximum output power).

The second device is an ICL designed at Université de Montpellier. This type of semiconductor lasers relies on interband transitions causing performance degradation at long wavelengths, which limits the room temperature operation at nearly 7 μm [31]. ICLs emitting in the transparency window around 4 μm can be considered for free-space experiments at room temperature. The ICL under investigation has a threshold current of 71 mA at 293 K and a maximum output power of 5.5 mW at 6.5 V and 250 mA, as displayed in Fig. 1(b). Even if the output power is lower than in the QCL's case, ICLs are envisioned for portable energy-efficient transmission systems because they usually consume less than 1 W of electrical power. Contrary to QCLs, ICLs exhibit relaxation oscillations above 1 GHz [32] but this will not affect our results because other phenomena degrade the bandwidth of the ICL under study, as shown hereafter. Contrary to the QCL under investigation, the ICL is not inserted in a HHL package and requires a cold finger to stabilize the temperature, as well as a focusing lens so that the beam can be analyzed with a detector.

B. Electrical and Optical Rectification

Prior to the experiments to determine the maximum data rate with the two semiconductor lasers, we assess the electrical bandwidth and the optical bandwidth of the lasers. For the electrical bandwidth, the method used is called rectification [33] and is depicted in Fig. 2. A frequency modulated (FM) signal made of a low-frequency tone (fixed at 2 kHz here) and a carrier frequency (varying between 10 MHz and 2000 MHz) is produced by a signal generator (Rohde&Schwarz SMIQ 06B) and subsequently sent towards the laser under study through the AC connector of

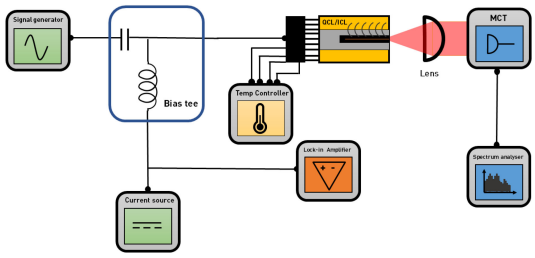

Fig. 2. Experimental setup for rectification, which is a method giving access to the electrical bandwidth and the optical bandwidth when using the lock-in amplifier and the MCT detector, respectively.

a bias-tee (bandpass filter between 0.1 MHz and 12 GHz). The non-linear LIV characteristics of the cascade laser generates a rectified current at the low-frequency tone that is proportional to the response at the carrier frequency. It is assumed that this response is the transfer function that governs the electrical carrier density under high-speed modulation. The rectified current is collected by the lock-in amplifier (EG&G Instruments 7220 DSP) connected to the DC port of the bias-tee (maximum DC current of 750 mA). It is thus possible to determine the electrical bandwidth of the two devices, as shown with the blue curves in Fig. 3. Generally, the laser under study is DC biased below optical threshold, in order to maximize the non-linear response and the rectified current retrieved by the lock-in amplifier. In our case, the electrical rectification was performed at 100 mA for the QCL while the current threshold is 515 mA and it was performed at 20 mA for the ICL while the current threshold is 71 mA. As we will study an optical transmission, it is also relevant to determine the optical bandwidth of the lasers and to compare it with the electrical bandwidth we retrieved with the rectification process. In this case, the laser is pumped above threshold and the synthesizer generates a sine wave with frequencies from 10 MHz to 2000 MHz. The optical signal emitted by the laser is then collected by a Mercury-Cadmium-Telluride (MCT Vigo PVI-4TE) detector with integrated amplifier and analyzed with an electrical spectrum analyzer working up to 43 GHz (Rohde&Schwarz FSU). The MCT detector has a 3-dB bandwidth of 700 MHz per manufacturer's specification. The result is depicted with red curves in Fig. 3 and shows a good agreement up to 1 GHz with the electrical rectification in the case of the QCL. In the case of the ICL, the electrical and the optical response are in accordance up to 300 MHz even if attenuation dips are stronger in the case of the electrical rectification. These discrepancies may be explained by the difference in pumping conditions, because an increase of the internal photon density is known to increase the response at high frequency [34]. From these two charts, one can see that neither the 700 MHz bandwidth of the MCT detector nor the relaxation oscillation of the ICL in the GHz range limit the transmission capabilities of the two lasers, since the response is already strongly attenuated below these frequencies in the two configurations.

C. High-Speed Modulation Experimental Setup

In the following, we will describe the transmission results for two different modulation formats: one is NRZ (non-return-to-zero) and the other one is RZ (return-to-zero) with 40 % duty cycle [35]. The NRZ signal is produced by a pattern generator (Hewlett Packard 70841 A) with data rates between 50 Mbits/s and 3000 Mbits/s while the RZ signal is generated by an arbitrary waveform generator (AWG Tektronix 7122B) with a sampling rate of 12 GS/s and an analog bandwidth of 3.5 GHz. For the RZ format, each each symbol is coded with 10 samples leading to a maximum symbol rate of 1200 Mbits/s. For both the NRZ format and the RZ format, the sequence used is a 127-bit long (2^7-1) pseudo-random bit signal (PRBS). The laser is pumped in CW mode with a low-noise current source (Wavelength Electronics QCL2000). The DC and AC signals are combined with a bias-tee prior to the connection to the laser's probes. In the case of the ICL, the maximum ouptut power is rather weak and, consequently, the beam is directly focused on the MCT detector that is placed one-meter away from the laser. In the case of the QCL, the light generated by the laser is sent towards a 50/50 beam splitter, so that part of the beam can be reflected by a mirror and this allows us to study the transmission resistance to unwanted external optical feedback. In order to adjust the feedback strength, a polarizer is placed in front of the mirror and is initially set in TE position to hinder back-reflection. The other beam coming from the 50/50 beam splitter is sent towards an MCT detector that is placed one-meter away from the laser. The QCL beam has a strong light intensity and a 20-dB optical attenuator followed by a polarizer is placed prior to the MCT detector to attenuate the beam and avoid MCT deterioration. Indeed, the MCT can detect mid-infrared AC signals down to an amplitude of a few dozens of μW and has a deterioration threshold of roughly 20 mW continuous power. The electrical AC output of the MCT is sent towards a low-noise oscilloscope (Tektronix MSO64) with a maximum sampling rate of 25 GS/s and an analog bandwidth of 2.5 GHz. The signal is also analyzed with an error detector (Hewlett Packard 70004 A) in the case of the NRZ format. An electrical switch allows displaying the two information without loss of electrical power. The error detector compares the bit of the seed PRBS signal with the bits of the received PRBS signal and allows recovering the real-time number of errors, contrary to post-analysis based on the shape and height of the eye diagram. The oscilloscope records the timetraces and a custom Matlab program resamples the data at a constant sample-per-bit ratio before plotting the eye diagrams. This program also determines the threshold leading to the lowest error rate and this is more accurate than the real-time error detector because the latter has an amplitude uncertainty of $\pm$ 5 mV. This detector however allows fast optimization without the need to record timetraces. The full setup in the case of the QCL experiment is shown in Fig. 4.

III. Evaluation of the Communication Channel

A. Transmission Results With QCL

As previously described, the main parameter to assess the quality of the transmission is the BER. Back in the 90s, communication with semiconductor lasers required BER below 10^{-11}. Forward Error Correction (FEC) was then successfully

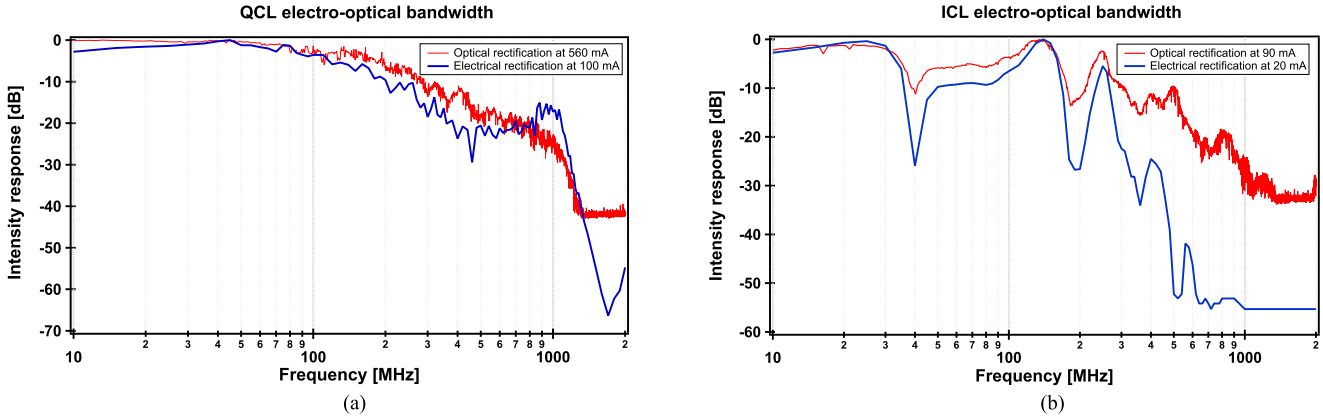

Fig. 3. Experimental rectification for (a) the QCL and (b) the ICL under study. For each chart, the optical rectification is printed in red and the electrical rectification is printed in blue. The two analyses are consistent in terms of cut-off frequency and local attenuation.

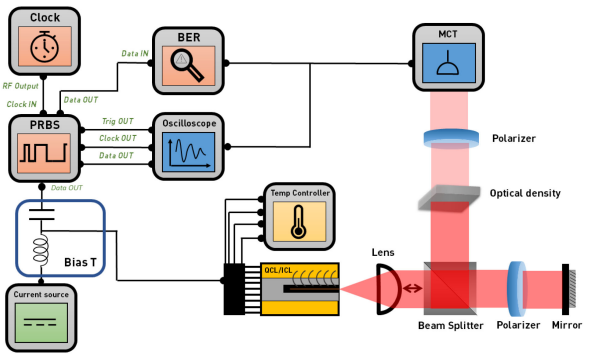

Fig. 4. Experimental setup for the free-space transmission, with a PRBS pattern generator and a error detector giving access to the BER. When the ICL (which emits less optical power than the QCL) is under study, the light beam goes directly to the MCT detector instead of being sent to the beam splitter and the optical attenuator.

introduced to improve the quality of recovery [36]. The price to pay, however, is a reduction of the data rate because, during the transmission, such correction requires additional bits, called overhead. The target BER determines the relevant FEC, which is characterized by its category, overhead length and decoding process. Continuous progress in FEC allows now getting rid of errors for a BER limit as high as 4×10^{-2} [37], that is called critical BER value in the following. This limit will be used to determine the maximum data rate when increasing the optical attenuation and when applying optical feedback. It is relevant to note that this critical value corresponds to a complicated soft-decision FEC threshold, which introduces high latency, and low BER values without correction are desirable. To complement our BER analysis, we display the eye diagram of the transmission. The latter is compared with the eye diagram of the initial bit sequence. An open eye in such diagrams can be related to the BER and the wider the eye, the lower the BER [38].

In the case of NRZ format, we are able to achieve a BER of 8×10^{-11} (measured with the error detector; no error found by the Matlab program within the recorded sequence) when the data rate is 400 Mbits/s, and the quality of the transmission can be visualized in Fig. 5(a). The eye is wide open and this means that one can perfectly discriminate '0' and '1' in the received signal. Our Matlab program confirms that the transmission is error-free, which means that the BER is lower than 10^{-4} considering the length of our recorded timetraces. This will serve as the reference value for each BER evaluation with the Matlab program. As previously explained, we want to increase the data rate while the transmission remains error-free when evaluated with the Matlab program, which is more accurate than our real-time error detector. The maximum rate we can achieve with the NRZ format is 546 Mbits/s and the corresponding eye diagram is displayed in Fig. 5(b). When further increasing the bit rate, the main issue comes from the decision threshold that is fixed for a given sequence. Indeed, one can see in Fig. 6(a) (top plot) that when at least two '1' bits are followed by a '0,' the optical response of the QCL is not sufficient to go below the decision threshold. Hence, the '0' bit will be considered as a '1' bit. The same conclusion is true for a long run of '0' bits followed by a single '1,' and this is detailed in the inset of Fig. 6(a). One of the options to mitigate this issue would be to use digital equalization at the receiver level [39]. Another option that is widely used in communication systems is to distort the seed signal with transmitter pre-emphasis [40], so that the aforementioned '0'bits (or '1'bits) actually have a response below (or above, respectively) the decision threshold. These methods are of utter interest and will be evaluated in future work. Instead, we decide to implement a more resistant modulation format because distortion is detrimental in our experiment, especially in the ICL's case. RZ patterns have shown relevant features in fiber transmissions [41], [42] and we decided to compare the performances of RZ and NRZ formats in our free-space configuration. One can see in Fig. 6(a) (bottom plot) that, for the same bit pattern and data transmission rate of 680 Mbits/s, the bits can now be discriminated with no error. The eye diagram of the corresponding seed signal and recovered message can be observed in Fig. 6(b). For the RZ case, the Matlab program confirms that the transmission is error-free, while in the NRZ case, the BER is 11%. The conclusion is that going from an NRZ format to an RZ format allows increasing the transmission rate from 546 Mbits/s to 680 Mbits/s while keeping an error-free communication.

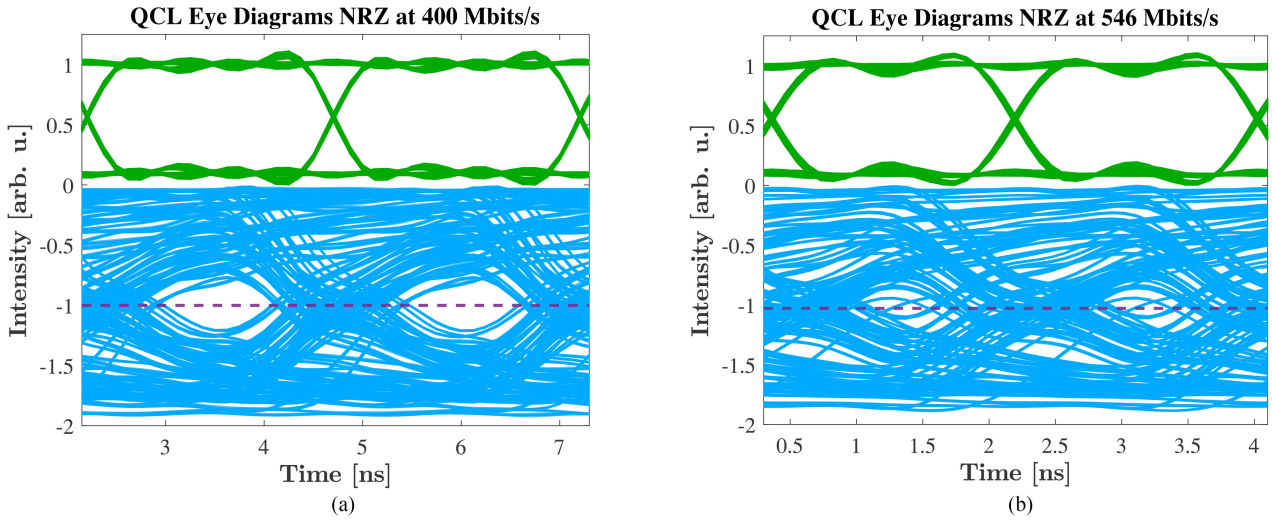

Fig. 5. Experimental eye diagrams retrieved for the QCL with an NRZ format at 400 Mbits/s (a) and 546 Mbits/s (b). The green trace corresponds to the seed signal while the blue trace corresponds to the transmitted signal and exhibits some degradation. At 546 Mbits/s, the degradation becomes quite detrimental. The purple dashed line is the threshold used by the Matlab program to compute errors.

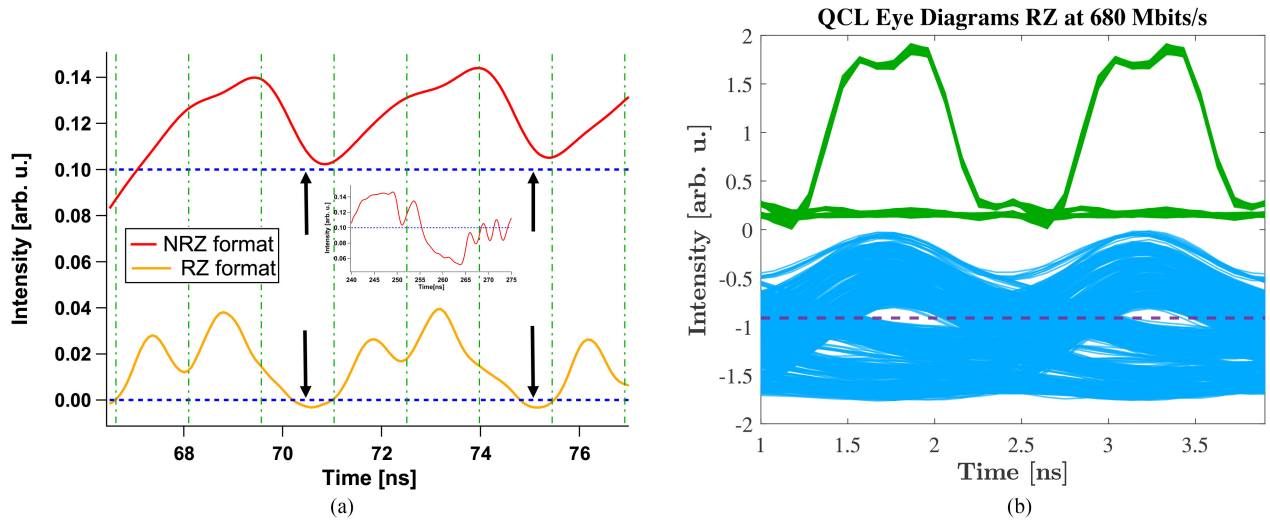

Fig. 6. (a) role of the RZ format in overcoming the threshold (dashed blue horizontal line) issue observed with the NRZ format at 680 Mbits/s; the bit sequence for the two traces (delimited by green dash-dot vertical lines) should be '1 101 101' but the black arrows show that only the RZ format translates correctly the '0' bits in this configuration. The inset demonstrates that changing the threshold level in the case of the NRZ format would be pointless because some of the bits, either '0' or '1,' fall outside the designated area. (b) Experimental eye diagrams retrieved for the QCL with an RZ format at 680 Mbits/s. The green trace corresponds to the seed signal while the blue trace corresponds to the transmitted signal. The purple dashed line is the threshold used by the Matlab program to compute errors.

B. Transmission Results With ICL

As observed from Fig. 3, the electrical and the optical bandwidth of the ICL are narrower than that of the QCL, so one can expect a lower transmission rate. Fig. 7(a) shows an open eye diagram for a data rate of 50 Mbits/s with NRZ format, even though jitter and small distortion play a role in degrading the shape of the eye. These two phenomena lead to an eye that is strongly deteriorated at 110 Mbits/s and this corresponds to the maximum rate we can achieve while keeping an error-free transmission (Fig. 7(b)). Even if this rate is five times lower than the one we achieved with QCL for the same format, it is relevant to remind that, up to date, only a 70 Mbits/s transmission was achieved with ICL and that experiment was carried out at 77 K [8] while our result is obtained at room temperature. Similarly to the case of QCL, we implement an RZ format in order to try to improve the data rate of the transmission. At 100 Mbits/s, the message is now clearly recovered because the pulses coding the bits are well separated, as detailed in Fig. 8(a). The maximum rate we were able to achieve while remaining error-free is 300 Mbits/s, and this results in clear improvement compared to the initial method with NRZ format. The corresponding eye diagram is depicted in Fig. 8(b) and shows that ICLs can be envisioned as energy-efficient mid-infrared sources for free-space communication, provided that the output power of such lasers is increased in the coming years. The major advantage of the RZ format

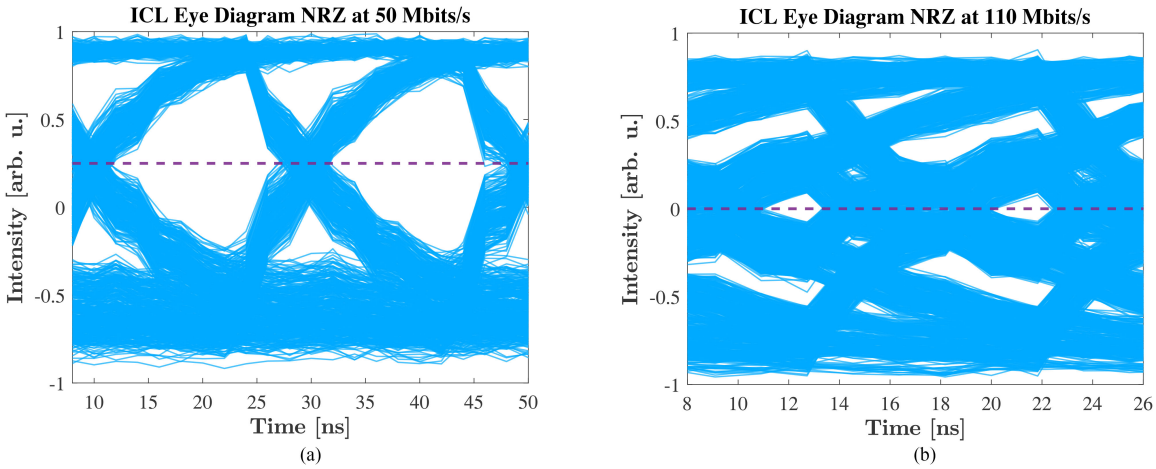

Fig. 7. Experimental eye diagrams retrieved for the ICL with an NRZ format at 50 Mbits/s (a) and 110 Mbits/s (b). The purple dashed line is the threshold used by the Matlab program to compute errors.

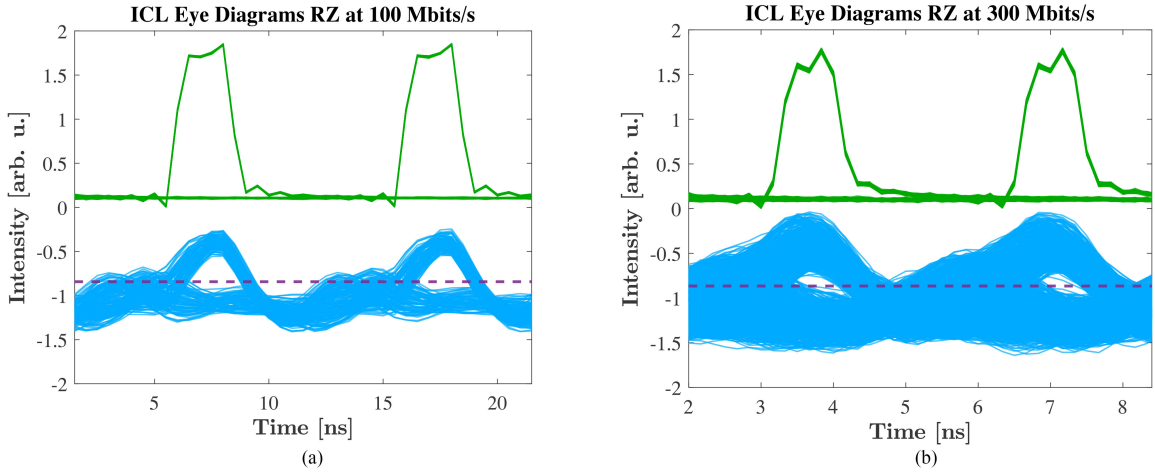

Fig. 8. Experimental eye diagrams retrieved for the ICL with an RZ format at 100 Mbits/s (a) and 300 Mbits/s (b). The purple dashed line is the threshold used by the Matlab program to compute errors.

in the ICL case could be explained by the strong attenuation around 40 MHz and around 200 MHz in the laser's response, which creates a bandpass filter. This improvement may only be compatible with short sequences, such as the 127-bit long pattern we used in the experiment.

C. Resistance to Perturbations

In the previous description of the QCL experiment, the attenuation between the laser facet and the MCT detector was set to 23 dB, with 3 dB coming from a 50/50 beam splitter and 20 dB coming from the optical attenuator. Subsequent attenuation will degrade the BER and this is what we evaluate in the configuration with a 400 Mbits/s NRZ format, as visualized in Fig. 9. With the initial 23 dB attenuation, we reach a BER lower than 10^{-10} with the error detector. By rotating the mid-infrared polarizer in front of the MCT detector, it is possible to increase the attenuation, which goes from 23 dB for a polarizer angle of 0° to 29 dB for a polarizer angle of 60°. When increasing the angle of the

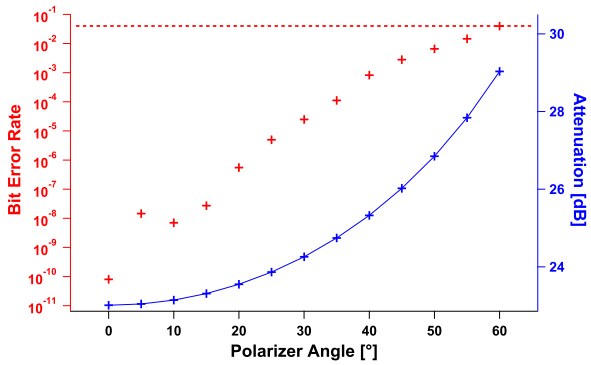

Fig. 9. Performance of the transmission with the QCL for a data rate of 400 Mbits/s. The red crosses represent the BER retrieved with the error detector when varying the polarizer angle in front of the MCT. The red dashed line corresponds to the critical BER value of 4×10^{-2}. The blue solid line is the total attenuation on the optical path (taking into account optical density and polarizer) as a function of the angle of the polarizer and shows that error correction codes could improve the transmission up to 29 dB attenuation.

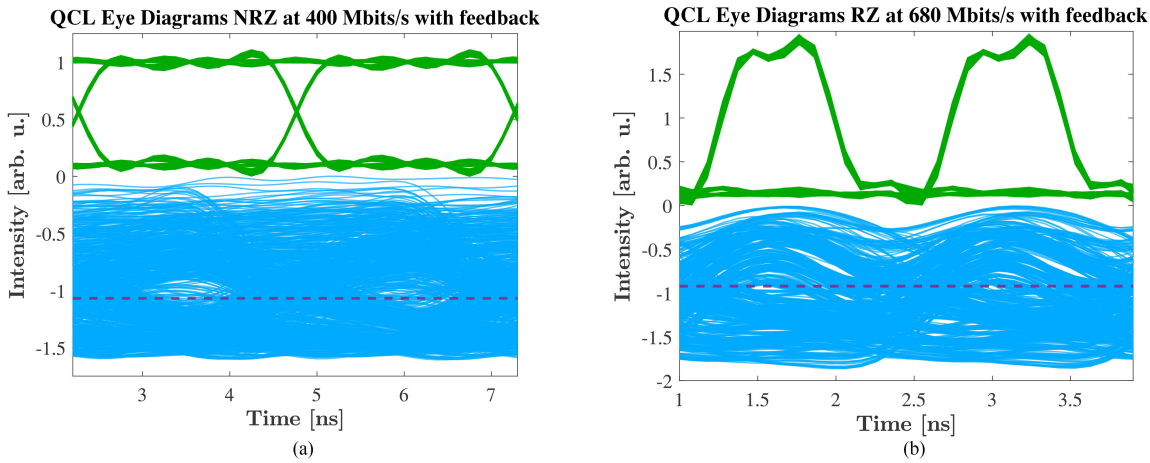

Fig. 10. Evaluation of the resistance to external optical feedback (a) for an NRZ-format at 400 Mbits/s and (b) for an RZ-format at 680 Mbits/s. Both traces were retrieved for an optical feedback ratio of 1% and show a degraded signal with a measured BER just above the critical value for the NRZ case, meaning that the signal is deteriorated beyond the FEC capabilities. The purple dashed line is the threshold used by the Matlab program to compute errors.

polarizer, the BER increases until it reaches a value of 4×10^{-2} at 60°, corresponding to an attenuation of 29 dB. This means that the transmission is effective up to 29 dB attenuation because with BER values below the critical level (dashed line in Fig. 9), it is possible to apply an overhead (i.e. extra signal bits) to correct errors. This finding is of utter interest for mid-infrared communication because a 29 dB attenuation corresponds to a free-space transmission of 4 km with a visibility of 600 meters [43] and the conclusion is that QCLs are candidates of choice even in degraded weather conditions.

The other perturbation we apply to the QCL is external optical feedback and that is dependent on the linewidth enhancement factor (LEF) of the laser under study. QCLs should theoretically exhibit a zero LEF [44] but, under actual operation, the LEF can amount to values between 2 and 3 [45]. Because of a lower LEF compared to conventional laser diodes [46], QCLs are renowned for being less sensitive to optical feedback when they are pumped with a continuous bias [47]. However, they are more likely to be destabilized when the electrical bias is modulated [48], and this case corresponds to our configuration where the current is modulated with a PRBS signal. The charts in Fig. 10 show the degradation of the BER when the QCL is subject to well-aligned external optical feedback, with a time delay of 2 ns. The behavior is very similar for the RZ signal and for the NRZ signal and the errors could not be corrected, even with 27 % overhead, for a feedback ratio of more than 1%. Though the configuration we study corresponds to a case where the feedback is accurately aligned and injected back into the laser cavity and this does not occur in realistic optical systems, the conclusion is that optical isolators are required in order to avoid parasitic feedback and unwanted BER degradation. These devices already exist in the mid-infrared domain and will be implemented when our system is integrated into a telescope for real-field long-distance transmissions.

IV. Conclusion

In summary, this work addresses free-space communication capabilities of two types of semiconductor lasers emitting in one of the transparency windows of the atmosphere. Our study shows that off-the-shelf packaged QCLs are compatible with high-speed long-distance transmissions with realistic optical attenuation. With an NRZ format, data rates up to 546 Mbits/s were achieved and with an RZ format, the rate was increased to 680 Mbits/s. The results we presented also showed the first free-space communication with a room-temperature ICL. The data rate of 110 Mbits/s obtained with an NRZ format was strongly improved by selecting an RZ format. This sets the maximum transmission speed at 300 Mbits/s and is promising for future experiments with these energy-efficient optical sources. The findings of our study can be implemented in applications where fiber deployment is rather difficult and expensive or when the emitter and receiver need to be mobile. The main advantage of this free-space scheme is its better resistance to atmospheric perturbation compared with communication at shorter wavelengths, while being directional. Further studies will focus on optimizing the RF injection at the level of the chip so that we can envision versatile easy-to-implement communication systems with multi-Gbits/s transmission rates. Improvements will also consider digital signal processing technique at the transmitter level and at the receiver level to comply with state-of-the-art communication procedures.

Acknowledgment

The Authors would like to thank Dr. Andreas Herdt's initial help to compute eye diagrams with Matlab and thank Dr. Elie Awwad for the fruitful discussions.

References

[1] J. Faist, F. Capasso, D. L. Sivco, C. Sirtori, A. L. Hutchinson, and A. Y. Cho, "Quantum cascade laser," *Science*, vol. 264, no. 5158, pp. 553–556, 1994.

[2] R. Q. Yang, "Infrared laser based on intersubband transitions in quantum wells," *Superlattices Microstructures*, vol. 17, no. 1, pp. 77–83, 1995.

[3] R. Martini *et al.*, "High-speed digital data transmission using mid-infrared quantum cascade lasers," *Electron. Lett.*, vol. 37, no. 21, pp. 1290–1292, 2001.

[4] C. Mann *et al.*, "Quantum cascade lasers for the mid-infrared spectral range: Devices and applications," in *Advances in Solid State Physics*, Springer-Verlag, Berlin Heidelberg, 2003, pp. 351–368.

[5] D. Hofstetter, M. Beck, and J. Faist, "Quantum-cascade-laser structures as photodetectors," *Appl. Phys. Lett.*, vol. 81, no. 15, pp. 2683–2685, 2002.
[6] D. Hofstetter, M. Beck, T. Aellen, and S. Blaser, "High-frequency modulation of a quantum-cascade laser using a monolithically integrated intracavity modulator," *IEEE Photon. Technol. Lett.*, vol. 15, no. 8, pp. 1044–1046, Aug. 2003.
[7] A. Soibel *et al.*, "High-speed operation of interband cascade lasers," *Electron. Lett.*, vol. 45, no. 5, pp. 264–265, 2009.
[8] A. Soibel *et al.*, "Midinfrared interband cascade laser for free space optical communication," *IEEE Photon. Technol. Lett.*, vol. 22, no. 2, pp. 121–123, Jan. 2010.
[9] F. Wang, S. Slivken, D. Wu, and M. Razeghi, "Room temperature quantum cascade lasers with 22% wall plug efficiency in continuous-wave operation," *Opt. Exp.*, vol. 28, no. 12, pp. 17532–17538, 2020.
[10] S. Pirotta *et al.*, "Fast amplitude modulation up to 1.5 GHz of mid-IR free-space beams at room-temperature," *Nat. Commun.*, vol. 12, no. 1, pp. 1–6, 2021.
[11] D. Palaferri *et al.*, "Room-temperature nine-μm-wavelength photodetectors and GHz-frequency heterodyne receivers," *Nature*, vol. 556, no. 7699, pp. 85–88, 2018.
[12] F. Kapsalidis *et al.*, "Mid-infrared quantum cascade laser frequency combs with a microstrip-like line waveguide geometry," *Appl. Phys. Lett.*, vol. 118, no. 7, 2021, Art. no. 071101.
[13] K. Pierściński *et al.*, "Butt-coupling of 4.5 μm quantum cascade lasers to silica hollow core anti-resonant fibers," *J. Lightw. Technol.*, vol. 39, no. 10, pp. 3284–3290, 2021.
[14] O. Spitz *et al.*, "Private communication with quantum cascade laser photonic chaos," *Nat. Commun.*, vol. 12, no. 1, pp. 1–8, 2021.
[15] A. Dunn *et al.*, "High-speed modulation of a terahertz quantum cascade laser by coherent acoustic phonon pulses," *Nat. Commun.*, vol. 11, no. 1, pp. 1–8, 2020.
[16] A. Khalatpour, A. K. Paulsen, C. Deimert, Z. R. Wasilewski, and Q. Hu, "High-power portable terahertz laser systems," *Nat. Photon.*, vol. 15, no. 1, pp. 16–20, 2021.
[17] M. Franckie, B. Meng, and J. Faist, "ZnO quantum cascade lasers for room temperature operation," in *Proc. SPIE*, vol. 11687, 2021, Art. no. 1168714.
[18] C. Liu *et al.*, "Free-space communication based on quantum cascade laser," *J. Semiconductors*, vol. 36, no. 9, 2015, Art. no. 094009.
[19] S. M. Johnson, E. Dial, and M. Razeghi, "High-speed free space optical communications based on quantum cascade lasers and type-II superlattice detectors," in *Proc. SPIE*, vol. 11288, 2020, Art. no. 1128814.
[20] X. Pang *et al.*, "Gigabit free-space multi-level signal transmission with a mid-infrared quantum cascade laser operating at room temperature," *Opt. Lett.*, vol. 42, no. 18, pp. 3646–3649, 2017.
[21] Y. H. Zhou *et al.*, "High-speed quantum cascade laser at room temperature," *Electron. Lett.*, vol. 52, no. 7, pp. 548–549, 2015.
[22] B. Hinkov, A. Hugi, M. Beck, and J. Faist, "Rf-modulation of mid-infrared distributed feedback quantum cascade lasers," *Opt. Exp.*, vol. 24, no. 4, pp. 3294–3312, 2016.
[23] H. Lotfi *et al.*, "High-frequency operation of a mid-infrared interband cascade system at room temperature," *Appl. Phys. Lett.*, vol. 108, no. 20, 2016, Art. no. 201101.
[24] P. Abramov, A. Budarin, E. Kuznetsov, and L. Skvortsov, "Quantum-cascade lasers in atmospheric optical communication lines: Challenges and prospects," *J. Appl. Spectrosc.*, vol. 87, no. 4, pp. 579–600, 2020.
[25] C. Colvero, M. Cordeiro, and J. P. Von Der Weid, "FSO systems: Rain, drizzle, fog and haze attenuation at different optical windows propagation," in *Proc. SBMO/IEEE MTT-S Int. Microw. Optoelectron. Conf.*, 2007, pp. 563–568.
[26] I. K. Son and S. Mao, "A survey of free space optical networks," *Digit. Commun. Netw.*, vol. 3, no. 2, pp. 67–77, 2017.
[27] A. Delga and L. Leviandier, "Free-space optical communications with quantum cascade lasers," in *Proc. SPIE*, vol. 10926, 2019, Art. no. 1092617.
[28] M. S. Vitiello, G. Scalari, B. Williams, and P. De Natale, "Quantum cascade lasers: 20 years of challenges," *Opt. Exp.*, vol. 23, no. 4, pp. 5167–5182, 2015.
[29] C. Wang, F. Grillot, V. I. Kovanis, J. D. Bodyfelt, and J. Even, "Modulation properties of optically injection-locked quantum cascade lasers," *Opt. Lett.*, vol. 38, no. 11, pp. 1975–1977, 2013.
[30] H. Lamela, B. Roycroft, P. Acedo, R. Santos, and G. Carpintero, "Experimental modulation bandwidth beyond the relaxation oscillation frequency in a monolithic twin-ridge laterally coupled diode laser based on lateral mode locking," *Opt. Lett.*, vol. 27, no. 5, pp. 303–305, 2002.
[31] J. Scheuermann *et al.*, "Single-mode interband cascade laser sources for mid-infrared spectroscopic applications," in *Proc. SPIE*, vol. 9855, 2016, Art. no. 98550G.
[32] Y. Deng and C. Wang, "Rate equation modeling of interband cascade lasers on modulation and noise dynamics," *IEEE J. Quantum Electron.*, vol. 56, no. 2, pp. 1–9, Apr. 2020.
[33] H. Liu, J. Li, M. Buchanan, and Z. Wasilewski, "High-frequency quantum-well infrared photodetectors measured by microwave-rectification technique," *IEEE J. Quantum Electron.*, vol. 32, no. 6, pp. 1024–1028, Jun. 1996.
[34] A. Calvar *et al.*, "High frequency modulation of mid-infrared quantum cascade lasers embedded into microstrip line," *Appl. Phys. Lett.*, vol. 102, no. 18, 2013, Art. no. 181114.
[35] P. J. Winzer and J. Leuthold, "Return-to-zero modulator using a single NRZ drive signal and an optical delay interferometer," *IEEE Photon. Technol. Lett.*, vol. 13, no. 12, pp. 1298–1300, Dec. 2001.
[36] F. Chang, K. Onohara, and T. Mizuochi, "Forward error correction for 100 G transport networks," *IEEE Commun. Mag.*, vol. 48, no. 3, pp. S48–S55, Mar. 2010.
[37] O. Ozolins *et al.*, "100 Gbaud PAM4 link without EDFA and post-equalization for optical interconnects," in *Proc. 45th Eur. Conf. Opt. Commun.*, IET, 2019, pp. 1–4.
[38] S. Gomez *et al.*, "High coherence collapse of a hybrid III-V/Si semiconductor laser with a large quality factor," *J. Physics: Photon.*, vol. 2, no. 2, 2020, Art. no. 025005.
[39] J. Liu and X. Lin, "Equalization in high-speed communication systems," *IEEE Circuits Syst. Mag.*, vol. 4, no. 2, pp. 4–17, 2004, doi: 10.1109/MCAS.2004.1330746.
[40] G. Belfiore, M. Khafaji, R. Henker, and F. Ellinger, "A 50 Gb/s 190 mW asymmetric 3-tap FFE VCSEL driver," *IEEE J. Solid-State Circuits*, vol. 52, no. 9, pp. 2422–2429, Sep. 2017.
[41] D. Breuer, K. Ennser, and K. Petermann, "Comparison of NRZ-and RZ-modulation format for 40 Gbit/s TDM standard-fibre systems," in *Proc. Eur. Conf. Opt. Commun.*, 1996, vol. 2, pp. 199–202.
[42] A. Yin, L. Li, and X. Zhang, "Analysis of modulation format in the 40 Gbit/s optical communication system," *Optik*, vol. 121, no. 17, pp. 1550–1557, 2010.
[43] C. Sauvage, C. Robert, B. Sorrente, F. Grillot, and D. Erasme, "Study of short and mid-infrared telecom links performance for different climatic conditions," in *Proc. SPIE*, vol. 11153, 2019, Art. no. 111530I.
[44] S. Bartalini *et al.*, "Observing the intrinsic linewidth of a quantum-cascade laser: Beyond the Schawlow-Townes limit," *Phys. Rev. Lett.*, vol. 104, no. 8, 2010, Art. no. 083904.
[45] O. Spitz *et al.*, "Extensive study of the linewidth enhancement factor of a distributed feedback quantum cascade laser at ultra-low temperature," in *Proc. SPIE*, vol. 10926, 2019, Art. no. 1092619.
[46] M. Osinski and J. Buus, "Linewidth broadening factor in semiconductor lasers-an overview," *IEEE J. Quantum Electron.*, vol. 23, no. 1, pp. 9–29, Jan. 1987.
[47] O. Spitz *et al.*, "Investigation of chaotic and spiking dynamics in mid-infrared quantum cascade lasers operating continuous-waves and under current modulation," *IEEE J. Sel. Topics Quantum Electron.*, vol. 25, no. 6, pp. 1–11, Nov./Dec. 2019.
[48] O. Spitz, J. Wu, M. Carras, C.-W. Wong, and F. Grillot, "Chaotic optical power dropouts driven by low frequency bias forcing in a mid-infrared quantum cascade laser," *Sci. Rep.*, vol. 9, no. 1, pp. 1–9, 2019.

Olivier Spitz was born in Besançon, France, on June 2, 1991. He received the Ph.D. degree in electrical engineering from Université Paris-Saclay, Gif-sur-Yvette, France, in 2019. He is currently a Postdoctoral Researcher with Télécom Paris, Palaiseau, France, working on applications of mid-infrared QCLs and ICLs. He is a Visiting Scholar with Electrical and Computer Engineering Department, University of California Los Angeles, Los Angeles, CA, USA, and with the Institut für Angewandte Physik, Technische Universität Darmstadt, Darmstadt, Germany. His research interests include nonlinear dynamics, free-space communications, and neuromorphic photonics. He is a Member of SPIE, OSA, and APS and has delivered more than 25 contributed talks at international conferences such as Photonics West, CLEO, IPC, and APS March Meeting among others.

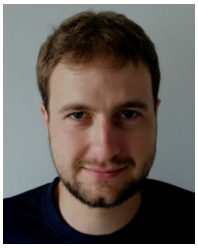

Pierre Didier was born in Paris, France, on April 14, 1996. He received the dual M.Sc. degrees in engineering from Grenoble INP–Phelma, Grenoble, France, and from Université Grenoble Alpes, Grenoble. He is currently working toward the Ph.D. degree with the group of Prof. Grillot, Télécom Paris, Palaiseau, France, with a focus on deploying free-space chaotic cryptography systems based on quantum cascade lasers and detectors. He was a Research Intern with Kungliga Tekniska Högskolan, Stockholm, Sweden, where he worked on X-ray photon detection using single photon semiconductor detectors. He was with Thales Research Laboratory, Palaiseau, France, on mid-infrared fiber lasers. His research interests include mid-infrared photonics, semiconductor components and communication systems.

Lauréline Durupt was born in France, in 1995. She received the M.Sc. degree in engineering from Grenoble INP–Phelma, Grenoble, France, Politecnico Di Torino, Turin, Italy and EPFL, Lausanne, Switzerland. She is currently working toward the Ph.D. degree with mirSense, Palaiseau, France, and she is involved in the development of novel semiconductor optical amplifiers and DFB laser for free-space communication issues (cFlow project). In 2020, she was a Junior Researcher with the group of Prof. Grillot, Télécom Paris, Palaiseau, France, working on optical feedback on mid-infrared quantum cascade laser and interband cascade laser.

Daniel Andrés Díaz-Thomas was born in Bogotá, Colombia, in 1993. He received the master's degree in physics and engineering of materials for microelectronics and nanotechnologies and the Ph.D. degree in 2020 in electronics from the University of Montpellier, Montpellier, France. His current research interests include GaSb and GaAs technologies for Mid-IR and THz optoelectronic devices.

Alexei N. Baranov received the Ph.D. degree in 1985 from the IOFFE Institute (Leningrad, USSR) and his Habilitation Diploma in 1996 from the University of Montpellier 2, Montpellier, France. From 1978 to 1993, he was with the IOFFE Institute as a Junior Researcher, Researcher, and Senior Researcher. In 1993, he joined the National Center for Scientific Research (CNRS), France and is currently the Research Director of Institut d'Electronique et des Systèmes, University of Montpellier, Montpellier, France. He pioneered mid-infrared antimonide-based photonics, participating in the very first developments in this field and later directing this research with the IOFFE Institute and with Montpellier. He guided innovative investigations resulting in the demonstration of novel types of mid-infrared semiconductor lasers, light-emitting diodes and photodetectors. He has more than 300 scientific publications, including more than 50 invited talks at international conferences. He is Editor of a book and author of four book chapters. His current research activity is focused on physics and technology of InAs-based quantum cascade lasers and interband cascade lasers. His research efforts have resulted in 20 patents on photonic devices and their technology. In 2006, his achievements in mid-infrared photonics have been recognized by the attribution of the Silver Medal of CNRS, one of the highest scientific awards in France. In 2017, he was elected Fellow of SPIE.

Laurent Cerutti was born in 1976. He received the Ph.D. degree from the University of Montpellier, Montpellier, France, in 2004. Then for a two year postdoctorate, he joined the Institute for Optoelectronic Systems and Microtechnology of the Polytechnic University of Madrid, Madrid, Spain, where he developed GaN nanowires grown on Si. Since 2006, he has been an Associate Professor with the University of Montpellier. He is author or coauthor of more than 100 publications in peer-reviewed journals, four books chapter and he coedited one book on Mid-Infrared Optoelectronics. His research activities focus on the development and the molecular beam epitaxy growth of Sb-based photonic devices, mainly for MIR VCSELs, lasers grown on Si, plasmonic structures, and interband cascade lasers.

Frédéric Grillot (Senior Member, IEEE) was born in Versailles, France, on August 22, 1974. He received the M.Sc. degree in physics from the University of Dijon, Dijon, France, in 1999, the Ph.D. degree in electrical engineering from the University of Besançon, Besançon, France, in 2003, and the Research Habilitation degree in physics from the University of Paris VII, Paris, France, in 2012. His doctoral research activities were conducted within the optical component research department at Nokia Bell Labs (formerly Alcatel-Lucent) working on the effects of the optical feedback dynamics in semiconductor lasers, and the impact this phenomenon has on communication systems. From 2003 to 2004, he was with the Center for Nanoscience and Nanotechnology, Université Paris-Saclay, Gif-sur-Yvette, France, where he focused on integrated optics modeling and silicon-based passive devices for optical interconnects. Between 2004 and 2012, he was an Assistant Professor with the Institut National des Sciences Appliquées, Rennes, France. From 2008 to 2009, he was a Visiting Research Professor with The University of New-Mexico, Albuquerque, NM, USA leading research in optoelectronics with the Center for High Technology Materials. In October 2012, he joined Télécom Paris, Palaiseau, France, one of the top public institutions of higher education and research of engineering in France as an Associate Professor and became Full Professor in January 2017. Since August 2015, he has also been a Research Professor with the University of New-Mexico. During April–December 2017, he joined the Electrical Engineering Department, University of California Los Angeles, Los Angeles, CA, USA, as a Visiting Professor teaching dynamics of lasers and applied quantum mechanics. He has authored or coauthored 90 journal articles, one book, three book chapters, and more than 200 contributions in international conferences and workshops. His current research interests include, but are not limited to, advanced quantum confined devices using new materials such as quantum dots and dashes, light emitters based on intersubband transitions, nonlinear dynamics and optical chaos in semiconductor lasers systems and microwave and silicon photonics applications. He is a Fellow Member of the SPIE, a Senior Member of the IEEE Photonics Society, and a Senior Member of the OSA.